



## White matter in different regions evolves differently during progression to dementia



Mahsa Dadar<sup>a,b,\*</sup>, Josefina Maranzano<sup>b,d</sup>, Simon Ducharme<sup>b,c</sup>, D. Louis Collins<sup>a,b</sup>, Alzheimer's Disease Neuroimaging Initiative<sup>1</sup>

<sup>a</sup>Neuroimaging and Surgical Tools Laboratory, Montreal Neurological Institute, McGill University, Montreal, Quebec, Canada

<sup>b</sup>McConnell Brain Imaging Centre, Montreal Neurological Institute, McGill University, Montreal, Quebec, Canada

<sup>c</sup>Department of Psychiatry, McGill University Health Centre, McGill University, Montreal, Quebec, Canada

<sup>d</sup>Department of Anatomy, University of Quebec in Trois-Rivieres, Trois-Rivieres, Quebec, Canada

### ARTICLE INFO

#### Article history:

Received 14 August 2018

Received in revised form 10 December 2018

Accepted 12 December 2018

Available online 21 December 2018

#### Keywords:

Small vessel disease

White matter hyperintensities

Dementia

Alzheimer's disease

Mild cognitive impairment

### ABSTRACT

White matter hyperintensities (WMHs) are common in individuals with mild cognitive impairment (MCI) and Alzheimer's disease. Patients with MCI with high WMH volumes are known to have an increased chance of conversion to Alzheimer's disease compared with those without WMHs. In this article, we assess the differences between patients with MCI that remain stable ( $N = 413$ ) and those that progress to dementia ( $N = 178$ ) in terms of WMH volume (as a surrogate of amount of tissue damage) and T1-weighted (T1w) image hypointensity (as a surrogate of severity of tissue damage) in periventricular, deep, and juxtacortical brain regions. Together, lesion volume and T1w hypointensity are used as a surrogate of vascular disease burden. Our results show a significantly greater increase of all regional WMH volumes in the MCI population that converts to dementia ( $p < 0.001$ ). T1w hypointensity for the juxtacortical WMHs was significantly lower in the converter group ( $p < 0.0001$ ) and was not affected by age. Conversely, T1w hypointensity in other regions showed a significant decrease with age ( $p < 0.0001$ ). Within the converters, Time2Conversion was associated with both WMH volume and T1w hypointensity ( $p < 0.0001$ ), and conversion to dementia was significantly associated with decreased intensity (and not volume) of periventricular and juxtacortical WMHs ( $p < 0.001$ ). These changes differ according to the WM region, suggesting that different mechanisms affect the juxtacortical area in comparison to deep and periventricular regions in the process of conversion to dementia.

© 2018 Elsevier Inc. All rights reserved.

### 1. Introduction

White matter hyperintensities (WMHs) are defined as nonspecific regions of higher intensity in the white matter (WM) tissue of the brain on T2w or Fluid-Attenuated Inversion Recovery (FLAIR) magnetic resonance (MR) images and are a common finding in the aging population in general, but also in individuals with vascular disease and other forms of dementia, including Alzheimer's disease (AD). WMHs are known to adversely impact cognitive function of

individuals without clinically significant symptoms and patients with mild cognitive impairment (MCI) and dementia (Yoshita et al., 2005). Therefore, WMHs are clinically important measures of vascular pathology that have diagnostic and prognostic value in the healthy aging, MCI, and AD populations (Bangen et al., 2018; Carmichael et al., 2010; De Groot et al., 2002; DeCarli et al., 2001; Dubois et al., 2014; Kandiah et al., 2014; Kim et al., 2015; Kloppenborg et al., 2014; Li et al., 2016; van den Berg et al., 2018; van Straaten et al., 2008). Several studies have assessed WMHs in individuals with MCI, reporting higher WMH volumes (particularly periventricular [PV] WMHs) in comparison with cognitively normal individuals, and an increased risk of developing MCI in healthy individuals with WMHs (DeCarli et al., 2001; Lopez et al., 2003). In addition, patients with MCI with high WMHs have a significantly higher chance of cognitive decline compared with patients without WMHs (Boyle et al., 2006; Kim et al., 2015; Lee et al., 2014; Li et al., 2016; Tosto et al., 2014). One study did not show such difference; however, they show that the changes in the Mahalanobis distance of WMH signal from normal-appearing WM using T1-weighted

\* Corresponding author at: Montreal Neurological Institute, 3801 University Street, Room WB320, Montréal, QC H3A 2B4. Tel.: 514-398-1573; fax: 514-398-8106.

E-mail address: [mahsa.dadar@mcgill.ca](mailto:mahsa.dadar@mcgill.ca) (M. Dadar).

<sup>1</sup> Part of the data used in preparation of this article was obtained from the Alzheimer's Disease Neuroimaging Initiative (ADNI) database ([adni.loni.usc.edu](http://adni.loni.usc.edu)). As such, the investigators within the ADNI contributed to the design and implementation of ADNI and/or provided data but did not participate in analysis or writing of this report. A complete listing of ADNI investigators can be found at: [http://adni.loni.usc.edu/wp-content/uploads/how\\_to\\_apply/ADNI\\_Acknowledgement\\_List.pdf](http://adni.loni.usc.edu/wp-content/uploads/how_to_apply/ADNI_Acknowledgement_List.pdf).

(T1w), T2w, and proton density–weighted MRI significantly differs between progressors and nonprogressors (Lindemer et al., 2015).

WMHs are MRI signs of small-vessel disease (SVD) related to chronic hypoperfusion and blood brain barrier alterations (McAleese et al., 2016). Their pathological substrate mainly reflects nonspecific demyelination, axonal loss, and higher levels of microglial activation (Gouw et al., 2010; Prins and Scheltens, 2015). In the past few decades, MRI studies with and without pathological correlates have assessed the differences in histopathology, risk factors, and clinical consequences of WMHs affecting the PV and deep WM regions (PV and deep WMHs) (DeBette and Markus, 2010; DeCarli et al., 2005; Huang et al., 2018; Krishnan et al., 2006). PV and deep WMHs are associated with different underlying pathologies and consequences and are thus often assessed separately. PV WMHs can be categorized into rims (surrounding the lateral ventricles) and caps (surrounding the anterior poles) (Kertesz et al., 1988). The pathologic findings associated with PV WMHs include myelin pallor, dilation of perivascular spaces, and increased extracellular spaces (Gouw et al., 2010). Deep WMHs are generally categorized into punctate and confluent lesions. They are frequently seen in the deep and subcortical WM on T2w and FLAIR MRIs of elderly individuals, particularly in those with vascular risk factors (Fazekas et al., 1993). They have been linked to chronic ischemia or brief and moderately severe repeated ischemia occurring in the subcortical WM (Jellinger et al., 2013; Matsusue et al., 2006).

A potential third compartment of WM that is less explored in the context of AD is juxtacortical short-range association fibers, known as U-fibers. These fibers are usually spared in the context of vascular pathology, a phenomenon attributed to the double vascularization of the area by the deep penetrating and pial perforating arteries (McAleese et al., 2016). In addition, the myelin component of these fibers has the lowest metabolic rate and completes the process of myelination at the latest stages of adulthood (Fornari et al., 2012). These differences in their biological characteristics makes the juxtacortical lesions (referred to here as JC WMHs) a potentially different category where the AD-related and vascular pathogenic mechanisms might have a different impact. In other words, it is an area that could be more preserved from a vascular pathology perspective. We have included this third category of JC WMHs because recent studies have shown that structural damage in the WM adjacent to the cortex (detected by semiquantitative MRI techniques) is associated with poorer performance in various cognitive tests in aging, MCI, and AD populations (Fornari et al., 2012; Gao et al., 2014; Nazeri et al., 2015).

In a previous study, we suggested that the hypointense regions observed on T1w images that are equivalent to the WMH regions on FLAIR and T2w images reflect the more severe spectrum of injury in the WM tissue and are associated with cognitive decline in cognitively normal patients and patients with MCI and AD (Dadar et al., 2018). The level of hypointensity on T1w images is another measure that might exhibit changes during progression to AD.

Although many studies have reported differences in WMH volumes between cognitively normal individuals and patients with MCI and AD as well as an increased risk of cognitive decline and conversion to AD in patients with high WMH volumes, it is still unclear whether there are significant longitudinal changes that occur in the volume or intensity of these lesions during the process of conversion that contribute to the cognitive decline. In this study, we aim to investigate whether there are specific changes in the WM (reflected in the intensity and volume of the lesions in different brain regions) of the individuals with MCI that occur during the process of conversion to dementia and whether these changes are associated with their cognitive decline. We hypothesize that (1) greater amount of WM disease burden (as measured by increased WMH volume, decrease in T1w

hypointensity, or a combination of both) occurs in the converter population in comparison to those that remain stable and (2) that this greater disease burden contributes to their greater cognitive decline and faster conversion to dementia.

## 2. Methods

### 2.1. Participants

Data used in this study include patients with MCI selected from the Alzheimer's Disease Neuroimaging Initiative (ADNI) database ([adni.loni.usc.edu](http://adni.loni.usc.edu)). The ADNI was launched in 2003 as a public-private partnership led by Principal Investigator Michael W. Weiner, MD. The primary goal of ADNI has been to test whether serial MRI, positron emission tomography, other biological markers, and clinical and neuropsychological assessment can be combined to measure the progression of MCI and early AD. ADNI was carried out with the goal of recruiting 800 adults aged from 55 to 90 years and consists of approximately 200 cognitively normal patients, 400 patients with MCI, and 200 patients with AD ([http://adni.loni.usc.edu/wp-content/uploads/2010/09/ADNI\\_GeneralProceduresManual.pdf](http://adni.loni.usc.edu/wp-content/uploads/2010/09/ADNI_GeneralProceduresManual.pdf)). ADNIGO is a later study that followed ADNI participants who were in cognitively normal or early MCI stages ([http://adni.loni.usc.edu/wp-content/uploads/2008/07/ADNI\\_GO\\_Procedures\\_Manual\\_06102011.pdf](http://adni.loni.usc.edu/wp-content/uploads/2008/07/ADNI_GO_Procedures_Manual_06102011.pdf)). ADNI2 study followed patients in the same categories, recruiting 550 new patients (<http://adni.loni.usc.edu/wp-content/uploads/2008/07/adni2-procedures-manual.pdf>). The longitudinal MRI data used in this study included T1w, T2w/proton density–weighted acquisitions from ADNI1 patients and T1w and FLAIR acquisitions from ADNI2/GO patients. The scanner information and image acquisition parameters have been previously described (Dadar et al., 2018).

### 2.2. Clinical evaluations

All patients received a comprehensive battery of clinical assessments and cognitive testing based on a standardized protocol (Petersen et al., 2010). At each visit, the participants underwent a series of assessments including Alzheimer's Disease Assessment Scale–Cognitive Subscale (ADAS–Cog). Patients with MCI are classified into converter/nonconverter cohorts based on the available clinical information in all follow-up visits; that is, the nonconverter cohort includes patients who have been consistently labeled MCI in all follow-up visits, whereas the converter cohort includes patients who at some point in the follow-up visits (mean follow-up:  $2.48 \pm 1.97$  y) convert to dementia and are labeled as dementia in all visits afterward. After this classification, 178 converters ( $N_{\text{Male}} = 112$ ) and 413 nonconverters ( $N_{\text{Male}} = 262$ ) were included in the study. Both groups had similar age (Age<sub>Converters</sub> =  $73.27 \pm 7.23$  years, Age<sub>Nonconverters</sub> =  $73.42 \pm 7.75$  years) and education levels (education<sub>converters</sub> =  $15.93 \pm 2.74$  years, education<sub>nonconverters</sub> =  $15.93 \pm 2.97$  years). Table 1 provides a summary of the descriptive characteristics separately for the converter and nonconverter cohorts used in this study.

### 2.3. WMH measurements

All MRI scans were preprocessed in 3 steps using our standardized pipeline: denoizing (Manjón et al., 2010), intensity inhomogeneity correction (Sled et al., 1998), and intensity normalization into the range 0–100. For each patient, the T2w, PD, and FLAIR scans were then coregistered to the structural T1w scan using a 6-parameter rigid registration and a mutual information objective function (Collins et al., 1994). The T1w scans were also registered to an average template based on ADNI patients (Collins

and Evans, 1997; Fonov et al., 2011). Using a previously validated fully automated WMH segmentation method and a library of manual segmentations based on 53 patients from ADNI1 and 46 patients from ADNI2/GO, the WMHs were automatically segmented in the patients with MCI for all longitudinal visits (i.e., multiple time points per individual) (Dadar et al., 2017a,b, 2018). The quality of the registrations and segmentations was visually assessed, and the results that did not pass this quality control were excluded ( $N_{\text{Total}} = 43$  out of 2773 time points for patients with MCI).

To assess the volumetric changes in different types of WMHs, the lesions were divided into 3 categories depending on their location: the PV, deep, and JC WMHs. To obtain WMH masks for each category, the whole-brain WMH masks were multiplied by 3 different masks:

- (1) A dilated (10<sup>mm</sup> dilation) ventricle mask to identify PV WMHs [similar to previous studies in the literature (DeCarli et al., 2005; Griffanti et al., 2017; Huang et al., 2018)].
- (2) A dilated gray matter mask (1<sup>mm</sup> dilation) for JC WMHs.
- (3) A WM mask excluding the previous 2 regions was used to identify Deep WMHs.

Fig. 1 shows an example of the 3 masks and WMHs from each of the 3 categories for one patient. The WMH volumes within each of these masks were calculated to obtain the total, PV, JC, and deep WMHs (all the volumetric information was calculated after normalization for intracranial volume). All volumes were then log-transformed to achieve a normal distribution.

To assess whether changes in T1w MRI intensity are associated with conversion to MCI, all longitudinal time points for each individual were linearly coregistered in the stereotaxic space and the

union of the WMH masks for different time points was obtained. The average T1w intensity of the WM tissue within (reflecting pathologic WM) and outside (reflecting normal WM) of this mask was measured, and the ratio of these 2 signals was calculated separately for PV, deep, and JC regions at each time point. This ratio is referred to as WM Abnormality Ratio (WMAR). WMAR values range between 0 and 1 and a lower WMAR value reflects greater abnormality. WMH volume reflects the size of the region of damage, whereas WMAR reflects the level of damage to the tissue. To simultaneously assess both, we define a third measure that we refer to as the overall burden of lesions (OBLs) as  $WMH\ volume * (1 - WMAR)$  for each region, where larger values indicate greater disease burden. An increase in OBL reflects either increase in WMH volume, decrease in WMAR, or both.

#### 2.4. Statistical analysis

To assess the differences between converter and nonconverter populations, a series of longitudinal mixed-effects models were used. The continuous fixed variables included age (or age at the baseline visit), WMH volume, and intensity measurements, Time2Conversion to AD (measured as the time from the current visit to the time point that the patient is diagnosed with dementia), and different cognitive scores. Sex, cohort (converter vs. non-converter MCI), and conversion (conversion from MCI to dementia, that is, the event of clinical diagnosis of dementia) were considered as categorical fixed variables. Subjects were considered as random effects. All continuous variables were z-scored in all the analyses. All statistical analysis was performed in MATLAB (version R2015b). Significant values after correction for multiple comparisons (Bonferroni correction) are indicated in bold font in all tables.

**Table 1**  
Descriptive statistics for the patients enrolled in this study

Measure	Converter	Nonconverter	p-value
Number of patients (N)	178	413	–
Original protocol	137/40	207/206	–
( $N_{\text{ADNI1}}/N_{\text{ADNI2/GO}}$ )			
Sex ( $N_{\text{Male}}/N_{\text{Female}}$ )	112/66	262/151	0.904
Baseline age (y)	73.27 ± 7.23	73.42 ± 7.75	0.934
Follow-up period (y)	2.55 ± 2.02	2.07 ± 2.01	<b>0.001</b>
Follow-up visits (N)	4.65 ± 2.10	4.18 ± 1.84	<b>&lt;0.0001</b>
Education (y)	15.93 ± 2.74	15.93 ± 2.97	0.958
Baseline ADAS-Cog13	20.44 ± 5.84	14.92 ± 6.38	<b>&lt;0.0001</b>
Baseline MMSE	26.80 ± 1.87	27.81 ± 1.82	<b>&lt;0.0001</b>
Baseline RAVLT-I	28.08 ± 6.92	36.05 ± 10.86	<b>&lt;0.0001</b>
Baseline RAVLT-F	5.05 ± 2.21	4.35 ± 2.58	<b>0.001</b>
Baseline RAVLT-L	2.85 ± 2.26	4.43 ± 2.68	<b>&lt;0.0001</b>
FAQ	5.17 ± 4.66	2.26 ± 3.33	<b>&lt;0.0001</b>
APOE4 ± (N)	118/59	175/237	<b>&lt;0.0001</b>
Vascular risk factors ± (N)	125/52	288/125	0.829
History of hypertension ± (N)	91/86	195/218	0.350
FDG	5.72 ± 0.55 (111)	6.36 ± 0.62 (314)	<b>&lt;0.0001</b>
AV45 amyloid beta (N)	1.39 ± 0.21 (39)	1.17 ± 0.20 (202)	<b>&lt;0.0001</b>
CSF Aβ 1–42 (N)	146.52 ± 37.43 (72)	174.94 ± 57.63 (102)	<b>0.0001</b>
CSF total tau	112.97 ± 51.42 (72)	94.64 ± 60.56 (102)	0.0382

Data are number or mean ± standard deviation. Vascular risk was determined by a yes/no question from the medical history information obtained during the participant's visit or a phone call. FDG indicates the average FDG-PET of angular, temporal, and posterior cingulate regions. AV45 indicates the average AV45 SUVR of frontal, anterior cingulate, precuneus, and parietal cortex relative to the cerebellum. p-values indicate group comparison results, determined by t-tests for continuous variables and  $\chi^2$  tests for categorical variables.

Bold font indicates significance after correction for multiple comparisons.

Key: ADNI, Alzheimer's disease neuroimaging initiative; ADAS-Cog, Alzheimer's disease assessment scale—cognitive subscale; APOE, apolipoprotein E; AV45, Florbetapir; CSF, cerebrospinal fluid; FDG, fluorodeoxyglucose; FAQ, functional assessment questionnaire; MMSE, mini-mental state examination; RAVLT, rey auditory verbal learning task (I, immediate; F, forgetting; L, learning); SUVR, standardized uptake value ratio.

### 3. Results

#### 3.1. Changes in WMH measures

To assess whether the changes of the 3 measures (WMH volume, WMAR, OBL) in each of the previously defined classes (deep, PV, JC) are different between converters and nonconverters, the following mixed-effects models were tested (Table 2).

Measure ~ 1 + Age \* Cohort + Sex + (1 | Subject).

The formula A\*B denotes A+B+A:B, where A and B are fixed variables (e.g., age and cohort here) and A:B is an interaction term between variables A and B. Measure denotes total, JC, deep or PV WMH volume, WMAR, or OBL, and cohort denotes converters against nonconverters. The volumetric results show significant interactions between cohort and age for all categories of WMHs ( $p < 0.002$ , indicating greater slopes/more increase in WMH volumes for the converter MCI cohort) as well as significant differences between converters and nonconverters in JC and deep WMH volumes ( $p < 0.006$ , indicating a higher overall volume of JC and deep WMHs for the converter MCIs). The WMAR results show a significant interaction between age and cohort for total, PV, and deep WMHs ( $p < 0.0001$ , indicating greater negative slopes/more decrease in WMAR, signifying more tissue damage for the converter MCI cohort). In contrast, JC WMARs appear to have significantly lower values for the converter cohort ( $p < 0.0001$ , indicating a lower overall WMAR/more tissue damage for the converter MCIs), without any significant relationship or interaction with age. The OBL results show a significant increase with age as well as a significant interaction between age and cohort for all regions ( $p < 0.0001$ , indicating increasing OBLs for both cohorts, with a greater slope/increase in the converter MCIs). In addition, JC OBLs have higher values for the converter cohort ( $p < 0.0001$ ). We did not observe any significant sex differences in any of the models.

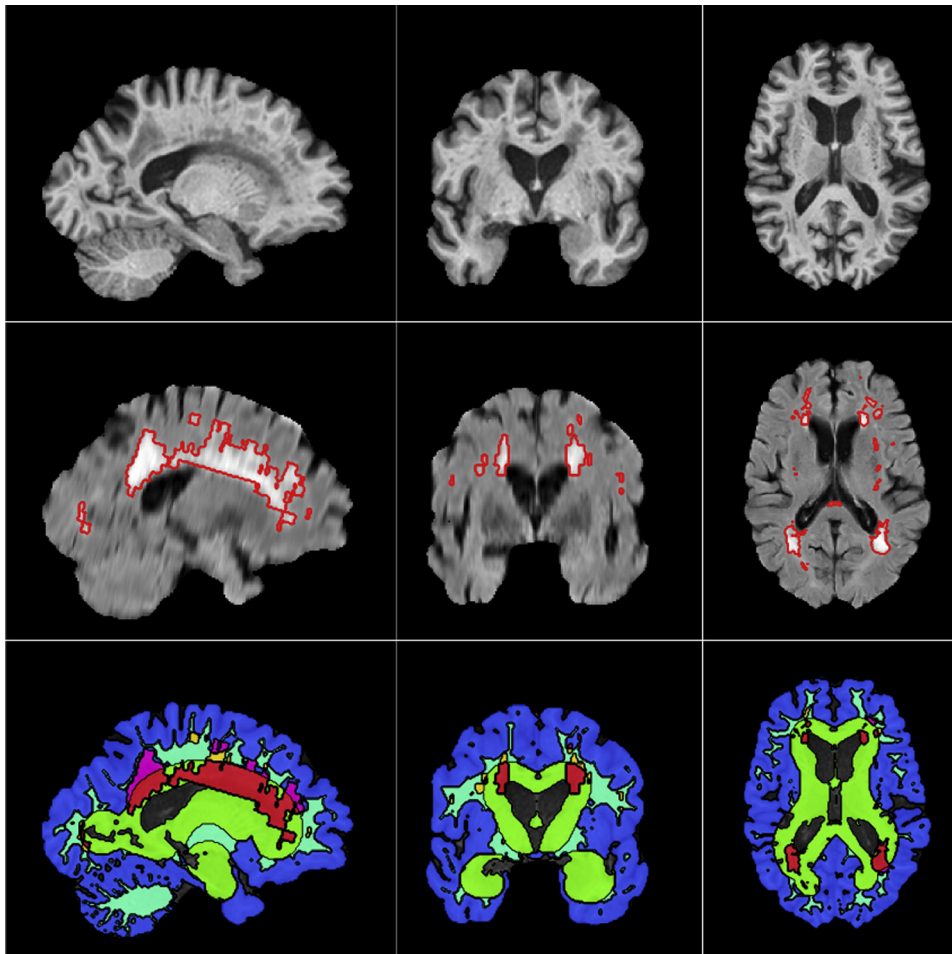


**Fig. 1.** An example of PV, deep, and JC WMH categorization for one individual. The first row shows sagittal, coronal, and axial slices of T1w images. The second row shows the same slices of FLAIR images with the WMHs contoured in red. The third row shows the 3 categories of WMHs. Blue: dilated GM mask (excluding JC WMHs). Cyan: deep WM mask (excluding deep WMHs). Green: PV mask (excluding PV WMHs). Red: PV WMHs. Magenta: JC WMHs. Orange: Deep WMHs. Abbreviations: FLAIR, FLuid-Attenuated Inversion Recovery; GM, gray matter; JC, juxtacortical; PV, periventricular; WMHs, white matter hyperintensities. (For interpretation of the references to color in this figure legend, the reader is referred to the Web version of this article.)

### 3.2. WMHs within converters

Within the converter group, we assessed whether the WMH changes were associated with time before conversion and whether

this relationship was different before and after conversion to dementia (Table 3).

Measure  $\sim 1 + \text{Time2Conversion} * \text{Conversion} + \text{Age\_baseline} + \text{Sex} + (1 | \text{Subject})$ .

**Table 2**  
Linear mixed-effects model: measure  $\sim 1 + \text{age} * \text{cohort} + \text{sex} + (1 | \text{Subject})$

Measure	Region	Total WMH		JC WMH		Deep WMH		PV WMH	
		Estimate	<i>p</i> -value						
Volume	Intercept	0.153	0.254	0.252	0.015	0.250	0.010	0.077	0.349
	Age	<b>1.042</b>	<b>&lt;0.0001</b>	<b>0.681</b>	<b>&lt;0.0001</b>	<b>0.568</b>	<b>&lt;0.0001</b>	<b>0.684</b>	<b>&lt;0.0001</b>
	Sex	-0.114	0.155	-0.149	0.0477	-0.138	0.058	-0.066	0.086
	Cohort	0.047	0.579	<b>0.206</b>	<b>0.006</b>	<b>0.217</b>	<b>0.004</b>	-0.015	0.849
	Age:Cohort	<b>0.477</b>	<b>&lt;0.001</b>	<b>0.295</b>	<b>&lt;0.0001</b>	<b>0.186</b>	<b>0.002</b>	<b>0.231</b>	<b>&lt;0.0001</b>
WMAR	Intercept	0.796	<0.0001	-0.146	0.101	-0.016	0.826	-0.268	0.091
	Age	<b>-0.093</b>	<b>&lt;0.0001</b>	-0.008	0.828	<b>-0.455</b>	<b>&lt;0.0001</b>	<b>-2.726</b>	<b>&lt;0.0001</b>
	Sex	0.008	0.167	-0.082	0.325	-0.083	0.345	0.303	0.040
	Cohort	-0.005	0.418	<b>-0.352</b>	<b>&lt;0.0001</b>	-0.088	0.335	-0.046	0.767
	Age:cohort	<b>-0.054</b>	<b>&lt;0.0001</b>	-0.023	0.645	<b>-0.327</b>	<b>&lt;0.0001</b>	<b>-1.540</b>	<b>&lt;0.0001</b>
OBL	Intercept	0.274	0.024	0.255	0.002	0.143	0.111	0.261	0.057
	Age	<b>2.145</b>	<b>&lt;0.0001</b>	<b>0.582</b>	<b>&lt;0.0001</b>	<b>0.721</b>	<b>&lt;0.0001</b>	<b>2.449</b>	<b>&lt;0.0001</b>
	Sex	-0.208	0.067	-0.034	0.660	0.008	0.921	-0.269	0.035
	Cohort	-0.106	0.368	<b>-0.358</b>	<b>&lt;0.0001</b>	-0.195	0.024	-0.048	0.719
	Age:cohort	<b>1.171</b>	<b>&lt;0.0001</b>	<b>0.320</b>	<b>&lt;0.0001</b>	<b>0.436</b>	<b>&lt;0.0001</b>	<b>1.331</b>	<b>&lt;0.0001</b>

Bold font indicates significant values after correction for multiple comparisons.

Key: JC, juxtacortical; OBL, overall burden of lesion; PV, periventricular; WMH, white matter hyperintensity; WMAR, white matter abnormality ratio.

The results show significant associations between WMH volumes in all categories and Time2Conversion ( $p < 0.002$ , indicating increase in volumes as the patient converts) and negative associations between total, and PV WMAR and Time2Conversion ( $p < 0.0001$ , indicating decrease in WMAR as the patients convert). The results show similar changes in WMH volumes with Time2Conversion, which remain relatively consistent after conversion (i.e., the event of Conversion and the interaction term Time2Conversion:Conversion are nonsignificant for all models, suggesting similar slopes of change in WMH volumes before and after conversion), while the PV and total WMH WMAR measures change significantly as the patients convert ( $p < 0.003$ , indicating a further decrease in both the intercept and slope of changes in WMAR/increased tissue damage after the patients convert to dementia). Similarly, the results show significant associations between OBL and Time2Conversion in all regions ( $p < 0.006$ ), as well as both a significant conversion ( $p < 0.0001$ ) and a significant interaction Time2Conversion:Conversion for PV and total OBL ( $p < 0.003$ ). We did not observe any significant sex differences in any of the models.

Note that the variable Time2Conversion has a negative value before the event of conversion occurs and a positive value after (see Fig. 2). Therefore, a positive association between WMH volume and Time2Conversion indicates an increase in the WMH volume as Time2Conversion increases (i.e., the patient nears and then passes the event of conversion). For example, here are the values for variables Conversion and Time2Conversion for a patient with 6 available visits with the following diagnosis and timeline:

Visit 1 at baseline: diagnosis = “MCI,” conversion = “not converted,” Time2Conversion = –1.5 years.

Visit 2 in 6 months: diagnosis = “MCI,” conversion = “not converted,” Time2Conversion = –1 year.

Visit 3 in 1 year: diagnosis = “MCI,” conversion = “not converted,” Time2Conversion = –0.5 years.

Visit 4 in 1.5 years: diagnosis = “MCI to dementia,” conversion = “converted,” Time2Conversion = 0 years.

Visit 5 in 2 years: diagnosis = “dementia,” conversion = “converted,” Time2Conversion = +0.5 years.

Visit 6 in 3 years: diagnosis = “dementia,” conversion = “converted,” Time2Conversion = +1.5 years.

Fig. 2 shows the overall trajectories estimated by the mixed-effects model and spaghetti plots for the individual patients for the 3 measures (i.e., WMH volume, WMAR, and OBL) for the whole

brain, as well as separately for JC, deep, and PV WM regions. Trajectories before and after conversion are shown in blue and red, respectively.

### 3.3. WMHs and cognition

Using mixed-effects models, we assessed the effect of WMH measures on changes in cognitive performance measured by the ADAS13 and their interactions with age and cohort, controlling for sex and years of education (Table 4).

ADAS13 ~ 1 + Sex + Education + Age\*WMH\* Cohort + (1 | Subject).

As expected, age was positively associated with ADAS13 in all models ( $p < 0.0001$ , note that a higher ADAS13 score indicates greater cognitive deficits). Education was negatively associated with ADAS13 in all models ( $p < 0.01$ ), suggesting an effect of cognitive reserve. We did not observe any significant sex differences in any of the models. There were significant associations between ADAS13 with WMH volumes, WMARs, and OBLs in all categories ( $p < 0.0001$ ). More interestingly, there were significant interactions between cohort and WMH volumes and OBL in all regions ( $p < 0.0003$ , indicating a greater effect of WMH volumes and the overall burden of the lesions on increasing cognitive deficits in the MCI converters), as well as total, deep, and PV WMAR ( $p < 0.0001$ ). The JC WMH volumes and OBL also had significant higher interactions with age and cohort ( $p < 0.0001$ ).

## 4. Discussion

In the present study, we considered 3 types of continuous MRI variables that reflect the burden of SVD: (1) WMH volume, capturing the overall lesion volume affecting the whole brain and the lesion volumes in 3 different regions: PV, deep, and JC WM; (2) the T1w signal decrease (WMAR), reflecting the level of the damage to the different WMHs areas; and (3) the OBL, reflecting a combination of the 2 previous measures. Our rationale for assessing the 3 WM compartments individually follows previous findings regarding the potential differences in PV and deep WMHs in terms of the associated underlying pathologies, that is, PV WMHs increase with arteriosclerosis, whereas deep WMHs increase with microinfarcts and cerebral hemorrhages (Shim et al., 2015).

**Table 3**

Linear mixed-effects model: measure ~ 1 + Time2Conversion\*conversion + age\_baseline + sex + (1 | Subject)

Measure	Region	Total WMH		JC WMH		Deep WMH		PV WMH	
		Estimate	p-value	Estimate	p-value	Estimate	p-value	Estimate	p-value
Volume	Intercept	0.004	0.980	–0.036	0.598	–0.012	0.656	–0.002	0.852
	Time2Conversion	<b>0.281</b>	<b>&lt;0.0001</b>	<b>0.232</b>	<b>&lt;0.0001</b>	<b>0.259</b>	<b>&lt;0.0001</b>	<b>0.168</b>	<b>&lt;0.0001</b>
	Conversion	0.047	0.043	0.063	0.167	0.093	0.080	0.005	0.898
	Time2Conversion:Conversion	0.004	0.872	0.001	0.998	–0.081	0.190	0.076	0.219
	Sex	0.092	0.513	–0.009	0.942	–0.016	0.896	0.101	0.458
	Age_baseline	<b>0.396</b>	<b>&lt;0.0001</b>	<b>0.314</b>	<b>&lt;0.0001</b>	<b>0.329</b>	<b>&lt;0.0001</b>	<b>0.346</b>	<b>&lt;0.0001</b>
WMAR	Intercept	0.198	<0.0001	0.091	0.222	0.008	0.910	0.208	0.001
	Time2Conversion	<b>–0.337</b>	<b>&lt;0.0001</b>	–0.002	0.897	<b>–0.099</b>	<b>&lt;0.0001</b>	<b>–0.449</b>	<b>&lt;0.0001</b>
	Conversion	<b>–0.280</b>	<b>&lt;0.0001</b>	<b>–0.083</b>	<b>0.001</b>	0.001	0.951	<b>–0.282</b>	<b>&lt;0.0001</b>
	Time2Conversion:Conversion	<b>–0.279</b>	<b>&lt;0.0001</b>	0.013	0.673	<b>–0.076</b>	<b>0.007</b>	<b>–0.343</b>	<b>&lt;0.0001</b>
	Sex	–0.043	0.741	0.130	0.396	–0.143	0.396	–0.117	0.316
	Age_baseline	<b>–0.173</b>	<b>0.005</b>	–0.078	0.279	–0.057	0.442	<b>–0.201</b>	<b>&lt;0.0001</b>
OBL	Intercept	–0.152	<0.0001	–0.078	0.275	–0.006	0.928	–0.169	0.009
	Time2Conversion	<b>0.400</b>	<b>&lt;0.0001</b>	<b>0.180</b>	<b>&lt;0.0001</b>	<b>0.218</b>	<b>&lt;0.0001</b>	<b>0.423</b>	<b>&lt;0.0001</b>
	Conversion	<b>0.218</b>	<b>&lt;0.0001</b>	0.088	0.024	0.019	0.573	<b>0.209</b>	<b>&lt;0.0001</b>
	Time2Conversion:conversion	<b>0.240</b>	<b>&lt;0.0001</b>	–0.004	0.919	0.037	0.356	<b>0.340</b>	<b>&lt;0.0001</b>
	Sex	0.086	0.510	–0.076	0.590	0.139	0.363	0.142	0.232
	Age_baseline	<b>0.308</b>	<b>&lt;0.0001</b>	<b>0.242</b>	<b>0.0002</b>	0.177	0.013	<b>0.310</b>	<b>&lt;0.0001</b>

Bold font indicates significant values after correction for multiple comparisons.

Key: JC, juxtacortical; OBL, overall burden of lesion; PV, periventricular; WMH, white matter hyperintensity; WMAR, white matter abnormality ratio.

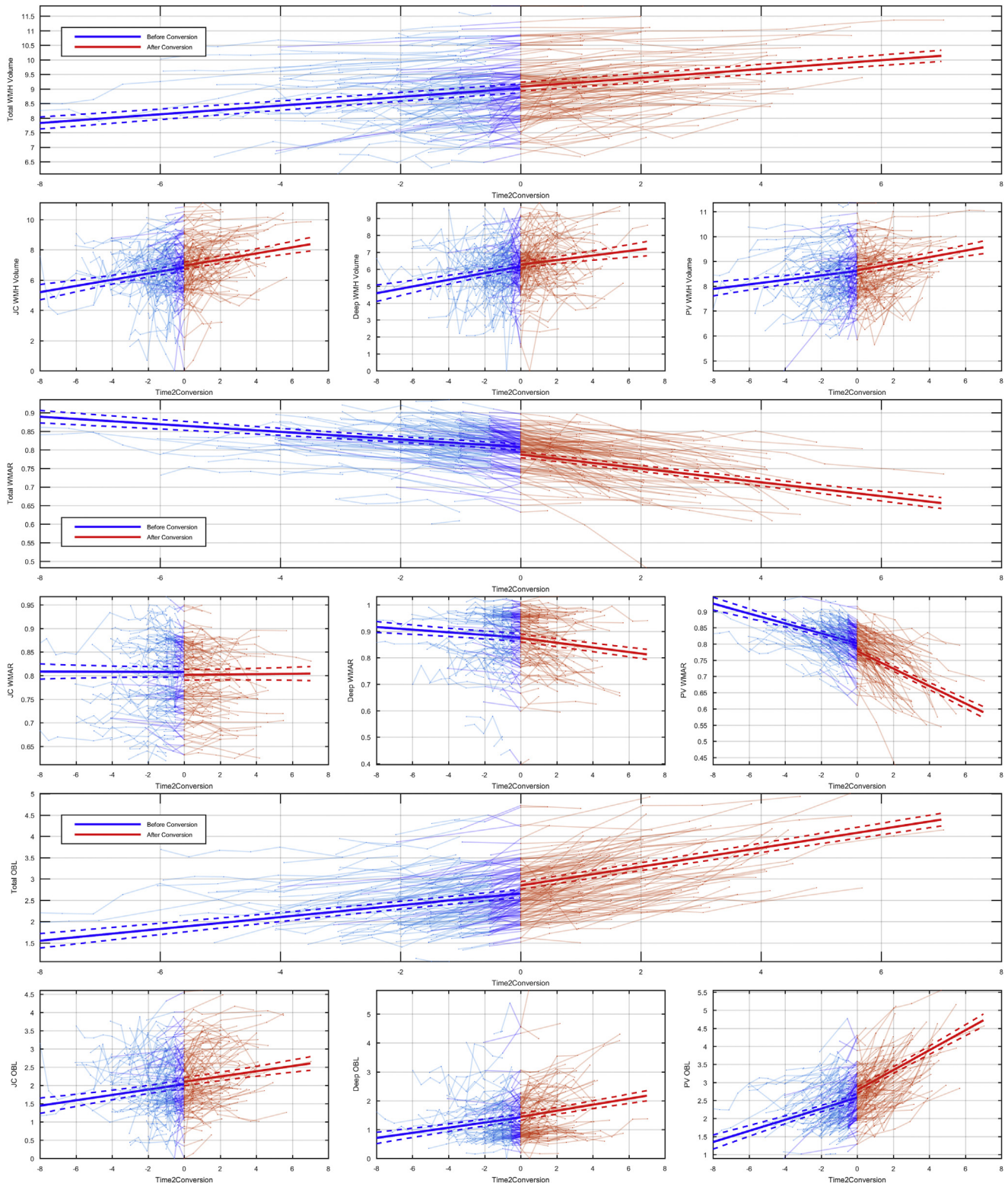


**Fig. 2.** Longitudinal WMH changes and conversion: Measure  $\sim 1 + \text{Time2Conversion} \times \text{Conversion} + (1 | \text{Subject})$ . All regional volumes are significantly associated with Time2Conversion. The total and PV WMAR seem to change significantly after the conversion event. WMH volumes are log-transformed. Abbreviations: AD, Alzheimer's disease; MCI, mild cognitive impairment; OBL, overall burden of lesions; Time2Conversion, Time from the current visit to the time point that the patient is diagnosed with AD (negative values for the years before the patient converts from MCI to AD, and positive afterward); PV, periventricular; WMAR, white matter abnormality ratio; WMH, white matter hyperintensities.

The third WM compartment (referred to here as JC WMHs) has been studied as a location of interest in aging and AD populations. Using magnetization transfer imaging to assess myelin in the JC

WM of patients with AD versus matched controls, Fornari et al. found significantly lower values in the AD cohort that were also associated with decline in various cognitive tests (Fornari et al.,

2012). Using diffusion tensor imaging and functional MRI, Gao et al. also described changes in the JC WM region (specifically in the short-range U-fibers), reporting that U-fibers were compromised in older participants and patients with AD. These changes were also associated with decreased performance in a prospective memory test (Gao et al., 2014).

Our results showed differences between the WMH measurements in the 3 compartments: the JC and deep WMH volumes were significantly higher in converter MCIs, and the JC WMAR discriminated the converters versus nonconverters (Table 2). Interestingly, age had a significant interaction with WMAR in all WMHs regions, except for the JC WMAR (Table 2), suggesting a potentially different mechanism affecting the JC regions compared to the PV and deep WM areas, which is more stable over time. This can be explained by the particular characteristics of the U-fibers, containing axons of pyramidal cells in layers III and V that are heavily affected in AD pathology, which complete myelination later in the human lifespan (Fornari et al., 2012; Gao et al., 2014) and whose metabolic rate is lower than other myelin regions in the nervous system. In addition, the PV and deep WM regions are supplied by nonoverlapping terminal arterioles with limited potential for collateral flow and a lower microvascular density compared with the gray matter and JC regions. This makes them more vulnerable to hypoperfusion and ischemic changes (Matsushita et al., 1994; Moody et al., 1990). We therefore speculate that the PV and deep WM areas could be more susceptible to vascular disease (in addition to AD pathology), whereas the JC areas would be relatively preserved from SVD-related injury.

WMH volumes were significantly associated with faster Time2Conversion to AD; that is, a positive association between

WMH volume and Time2Conversion (as is the case for all regional WMH volumes) implies an increase in WMH volume as time passes (Time2Conversion increases) (Table 3). In addition, having a higher severity of WM lesions (as measured by WMARs) was associated with a shorter Time2Conversion in the converters, except for JC WMAR; that is, negative association between WMAR and Time2Conversion (as is the case for all regional WMARs) indicates more abnormality in WMAR (because lower WMAR values reflect greater abnormality) as time passes. This could be interpreted as a slower changing process taking place at the JC level, as opposed to the more rapid changes occurring in the PV and deep WM areas (Table 3). This again reinforces the idea of a different injury mechanism taking place in the JC WMHs versus the PV and deep WMHs. In addition, while the rate of WMH volume increase remained consistent before and after conversion to AD, the WMAR rate showed a significant change after conversion to AD, suggesting that while the rate of increase in lesion volume does not significantly change, the amount of WM damage in these lesions is greater after conversion to AD. This is also reflected in the increasing slope of the OBL metric after conversion to AD, driven mostly by the PV lesions.

Finally, we evaluated the association between cognitive performance and the WMH measurements along with age, sex, education, and the converter status. ADAS13 was significantly associated with the WMH measures in all WM compartments (Table 4). More interestingly, the converter cohort has a significant interaction with the WMH measures, indicating their higher contribution to cognitive decline in this cohort. This further underlines the clinical relevance of the WMH assessments in relation to cognitive decline in the MCI population.

**Table 4**  
Linear mixed-effects model: ADAS13 ~ 1 + sex + education + age\*WMH\* cohort + (1 | Subject)

Measure	Total WMH		JC WMH		Deep WMH		PV WMH	
	Estimate	p-value	Estimate	p-value	Estimate	p-value	Estimate	p-value
<b>Volume</b>								
Intercept	0.612	<0.0001	0.613	<0.0001	0.642	<0.0001	0.731	<0.0001
Age	<b>0.702</b>	<b>&lt;0.0001</b>	<b>0.966</b>	<b>&lt;0.0001</b>	<b>1.029</b>	<b>&lt;0.0001</b>	<b>1.063</b>	<b>&lt;0.0001</b>
Sex	-0.065	0.388	-0.048	0.518	-0.059	0.435	-0.081	0.292
Education	<b>-0.104</b>	<b>0.003</b>	<b>-0.106</b>	<b>0.002</b>	<b>-0.101</b>	<b>0.004</b>	<b>-0.105</b>	<b>0.003</b>
Vol	<b>0.640</b>	<b>&lt;0.0001</b>	<b>0.236</b>	<b>&lt;0.0001</b>	<b>0.240</b>	<b>&lt;0.0001</b>	<b>0.228</b>	<b>&lt;0.0001</b>
Cohort	<b>0.968</b>	<b>&lt;0.0001</b>	<b>-0.964</b>	<b>&lt;0.0001</b>	<b>0.979</b>	<b>&lt;0.0001</b>	<b>-1.066</b>	<b>&lt;0.0001</b>
Age:vol	0.086	0.011	0.129	0.068	<b>0.063</b>	<b>0.002</b>	-0.071	0.025
Age:cohort	<b>0.513</b>	<b>&lt;0.0001</b>	<b>0.764</b>	<b>&lt;0.0001</b>	<b>0.822</b>	<b>&lt;0.0001</b>	<b>0.840</b>	<b>&lt;0.0001</b>
Vol:cohort	<b>0.541</b>	<b>&lt;0.0001</b>	<b>0.162</b>	<b>0.0003</b>	<b>0.174</b>	<b>&lt;0.0001</b>	<b>0.199</b>	<b>&lt;0.0001</b>
Age:vol:cohort	0.047	0.297	<b>0.115</b>	<b>0.005</b>	0.067	0.079	0.089	0.034
<b>WMAR</b>								
Intercept	0.586	<0.0001	0.668	<0.0001	0.687	<0.0001	0.600	<b>&lt;0.0001</b>
Age	<b>0.389</b>	<b>&lt;0.0001</b>	<b>1.205</b>	<b>&lt;0.0001</b>	<b>1.156</b>	<b>&lt;0.0001</b>	<b>0.211</b>	<b>&lt;0.0001</b>
Sex	-0.023	0.719	-0.059	0.458	-0.088	0.272	-0.017	0.777
Education	<b>-0.112</b>	<b>0.0001</b>	<b>-0.109</b>	<b>0.003</b>	-0.095	0.012	<b>-0.122</b>	<b>&lt;0.0001</b>
WMAR	<b>-0.958</b>	<b>&lt;0.0001</b>	<b>-1.004</b>	<b>&lt;0.0001</b>	<b>-1.005</b>	<b>&lt;0.0001</b>	<b>-0.982</b>	<b>&lt;0.0001</b>
Cohort	<b>0.553</b>	<b>&lt;0.0001</b>	0.095	0.033	<b>0.341</b>	<b>&lt;0.0001</b>	<b>0.535</b>	<b>&lt;0.0001</b>
Age: WMAR	<b>-0.200</b>	<b>0.001</b>	<b>-0.972</b>	<b>&lt;0.0001</b>	<b>-0.924</b>	<b>0&lt;0.0001</b>	-0.028	0.637
Age:cohort	<b>0.061</b>	<b>0.001</b>	<b>0.118</b>	<b>0.004</b>	0.059	0.154	<b>0.067</b>	<b>&lt;0.0001</b>
WMAR:cohort	<b>-0.484</b>	<b>&lt;0.0001</b>	-0.084	0.148	<b>-0.316</b>	<b>&lt;0.0001</b>	<b>-0.468</b>	<b>&lt;0.0001</b>
Age: WMAR:cohort	-0.027	0.359	<b>-0.115</b>	<b>0.029</b>	-0.024	0.630	-0.018	0.492
<b>OBL</b>								
Intercept	0.543	<0.0001	0.588	<0.0001	0.637	<0.0001	0.591	<0.0001
Age	<b>0.180</b>	<b>0.001</b>	<b>0.947</b>	<b>&lt;0.0001</b>	<b>0.947</b>	<b>&lt;0.0001</b>	<b>0.158</b>	<b>0.002</b>
Sex	-0.021	0.729	-0.034	0.638	-0.068	0.361	-0.024	0.692
Education	<b>-0.112</b>	<b>0.0001</b>	<b>-0.108</b>	<b>0.001</b>	<b>-0.097</b>	<b>0.005</b>	<b>-0.122</b>	<b>&lt;0.0001</b>
OBL	<b>-0.924</b>	<b>&lt;0.0001</b>	<b>-0.933</b>	<b>&lt;0.0001</b>	<b>-0.967</b>	<b>&lt;0.0001</b>	<b>-0.975</b>	<b>&lt;0.0001</b>
Cohort	<b>0.656</b>	<b>&lt;0.0001</b>	<b>0.228</b>	<b>&lt;0.0001</b>	<b>0.338</b>	<b>&lt;0.0001</b>	<b>0.585</b>	<b>&lt;0.0001</b>
Age: OBL	-0.019	0.760	<b>-0.737</b>	<b>&lt;0.0001</b>	<b>-0.734</b>	<b>&lt;0.0001</b>	0.016	0.798
Age:cohort	<b>0.070</b>	<b>0.0002</b>	<b>0.149</b>	<b>&lt;0.0001</b>	0.077	0.025	<b>0.057</b>	<b>0.001</b>
OBL:cohort	<b>-0.550</b>	<b>&lt;0.0001</b>	<b>-0.155</b>	<b>0.001</b>	<b>-0.265</b>	<b>&lt;0.0001</b>	<b>-0.5062</b>	<b>&lt;0.0001</b>
Age: OBL:cohort	-0.029	0.347	<b>-0.150</b>	<b>0.0006</b>	-0.075	0.097	-0.008	0.761

Bold font indicates significant values after correction for multiple comparisons.

Key: JC, juxtacortical; OBL, overall burden of lesion; PV, periventricular; WMH, white matter hyperintensity; WMAR, white matter abnormality ratio.

Because the main question of interest in this study was to investigate the patterns of change in different WMH measures and their relationship with cognitive decline in individuals with MCI, the converter cohort includes all patients with MCI who convert to dementia, not necessarily AD dementia ( $N = 178$ ). However, limiting the converter cohort to only patients with a confirmed diagnosis of AD dementia ( $N = 118$ ), we found similar results in all analyses (supplementary materials [Tables S1–S3](#)).

Our study has several limitations, the main one being the lack of quantitative MRI pulse sequences to assess the different WM areas. Adding information from magnetization transfer imaging or T1 mapping techniques could give more insight to the potential changes in regional WMHs. Similarly, histopathology data of WMH areas would provide essential information, mainly of the JC area, which has not been the subject of extensive assessment in studies correlating *ex vivo* MRI WMHs and histology analysis in the AD population.

Most studies either assess the total burden of WMHs or classify them into PV and deep categories. Separating JC WMHs from the deep WMHs, we observed differences in their behavior from the PV and deep WMHs. These differences are evident when assessing traditional MRI pulse sequences that allow the quantification of T2w/FLAIR WMHs volumes and T1w WMHs intensity values.

Because several vascular risk factors are treatable, prevention and treatment of factors that are associated with WMHs is currently one of the main recommendations to slow cognitive decline ([Leshner et al., 2017](#)). One of the most important strategies regarding reduction of vascular disease risk and consequently WMH burden has been to control hypertension, which subsequently reduces the risk of cognitive decline ([de Leeuw et al., 2002](#); [DeBette and Markus, 2010](#); [Dufouil et al., 2001, 2005](#); [Edwards et al., 2017](#)). Further assessment of WMHs in the JC, PV, and deep compartments in these types of patients (hypertensive controlled with medication) could increase the insight into the susceptibility of injury mediated by SVD in the different brain regions.

In summary, our results show that the WMHs in different regions of the brain evolve differently in the process of conversion to AD. Although PV and deep WMHs showed more pronounced changes during the process of conversion, the JC WMAR significantly differed between the converter and nonconverter groups. The significant changes in the WMAR in PV regions after conversion indicate that increased damage to the tissue (and not increased size of the regions of damage) is related to disease progression.

## Disclosure

MD and JM have no conflicts of interest to report. SD receives salary funding from the Fonds de Recherche du Québec—Santé. DLC reports grants from Canadian Institutes of Health Research, National Science and Engineering Research Council, Canadian foundation for Innovation, and other from NeuroRx Inc and True Positive Medical Devices, during the conduct of the study.

## Acknowledgements

The authors would like to acknowledge funding from the Famille Louise & André Charron. This work was also supported by grants from the Canadian Institutes of Health Research (MOP-111169), les Fonds de Recherche Santé Québec Pfizer Innovation fund, an NSERC CREATE grant (4140438 - 2012), the Levesque Foundation, the Douglas Hospital Research Centre and Foundation, the Government of Canada, and the Canada Fund for Innovation. This research was also supported by NIH grants P30AG010129, K01 AG030514, and the Dana Foundation.

Data collection and sharing for this project was funded by the Alzheimer's Disease Neuroimaging Initiative (ADNI), United States (National Institutes of Health, United States Grant U01 AG024904) and DOD ADNI (Department of Defense, United States award number W81XWH-12-2-0012). ADNI is funded by the National Institute on Aging, United States, the National Institute of Biomedical Imaging and Bioengineering, United States, and through generous contributions from the following: AbbVie, Alzheimer's Association; Alzheimer's Drug Discovery Foundation; Araclon Biotech; BioClinica, Inc; Biogen; Bristol-Myers Squibb Company; CereSpir, Inc; Cogstate; Eisai Inc; Elan Pharmaceuticals, Inc; Eli Lilly and Company; EuroImmun; F. Hoffmann-La Roche Ltd and its affiliated company Genentech, Inc; Fujirebio; GE Healthcare; IXICO Ltd; Janssen Alzheimer Immunotherapy Research & Development, LLC.; Johnson & Johnson Pharmaceutical Research & Development LLC.; Lumosity; Lundbeck; Merck & Co, Inc; Meso Scale Diagnostics, LLC.; NeuroRx Research; Neurotrack Technologies; Novartis Pharmaceuticals Corporation; Pfizer Inc; Piramal Imaging; Servier; Takeda Pharmaceutical Company; and Transition Therapeutics. The Canadian Institutes of Health Research is providing funds to support ADNI clinical sites in Canada. Private sector contributions are facilitated by the Foundation for the National Institutes of Health ([www.fnih.org](http://www.fnih.org)). The grantee organization is the Northern California Institute for Research and Education, and the study is coordinated by the Alzheimer's Therapeutic Research Institute at the University of Southern California. ADNI data are disseminated by the Laboratory for Neuro Imaging at the University of Southern California.

## Appendix A. Supplementary data

Supplementary data associated with this article can be found, in the online version, at <https://doi.org/10.1016/j.neurobiolaging.2018.12.004>.

## References

- Bangen, K.J., Preis, S.R., Delano-Wood, L., Wolf, P.A., Libon, D.J., Bondi, M.W., Au, R., DeCarli, C., Brickman, A.M., 2018. Baseline white matter hyperintensities and hippocampal volume are associated with conversion from normal cognition to mild cognitive impairment in the framingham offspring study. *Alzheimer Dis. Assoc. Disord.* 32, 50–56.
- Boyle, P.A., Wilson, R.S., Aggarwal, N.T., Tang, Y., Bennett, D.A., 2006. Mild cognitive impairment risk of Alzheimer disease and rate of cognitive decline. *Neurology* 67, 441–445.
- Carmichael, O., Schwarz, C., Drucker, D., Fletcher, E., Harvey, D., Beckett, L., Jack, C.R., Weiner, M., DeCarli, C., 2010. Longitudinal changes in white matter disease and cognition in the first year of the Alzheimer disease neuroimaging initiative. *Arch. Neurol.* 67, 1370–1378.
- Collins, D.L., Evans, A.C., 1997. Animal: validation and applications of nonlinear registration-based segmentation. *Int. J. Pattern Recognit. Artif. Intell.* 11, 1271–1294.
- Collins, D.L., Neelin, P., Peters, T.M., Evans, A.C., 1994. Automatic 3D intersubject registration of MR volumetric data in standardized Talairach space. *J. Comput. Assist. Tomogr.* 18, 192–205.
- Dadar, M., Maranzano, J., Ducharme, S., Carmichael, O.T., Decarli, C., Collins, D.L., Initiative, A.D.N., 2018. Validation of T1w-based segmentations of white matter hyperintensity volumes in large-scale datasets of aging. *Hum. Brain Mapp.* 39, 1093–1107.
- Dadar, M., Maranzano, J., Misquitta, K., Anor, C.J., Fonov, V.S., Tartaglia, M.C., Carmichael, O.T., Decarli, C., Collins, D.L., Alzheimer's Disease Neuroimaging Initiative, 2017a. Performance comparison of 10 different classification techniques in segmenting white matter hyperintensities in aging. *Neuroimage* 157, 233–249.
- Dadar, M., Pascoal, T., Manitsirikul, S., Misquitta, K., Tartaglia, C., Brietner, J., Rosa-Neto, P., Carmichael, O., Decarli, C., Collins, D.L., 2017b. Validation of a regression technique for segmentation of white matter hyperintensities in Alzheimer's disease. *IEEE Trans. Med. Imaging* 36, 1758–1768.
- De Groot, J.C., De Leeuw, F.-E., Oudkerk, M., Van Gijn, J., Hofman, A., Jolles, J., Breteler, M., 2002. Periventricular cerebral white matter lesions predict rate of cognitive decline. *Ann. Neurol.* 52, 335–341.

- de Leeuw, F.E., de Groot, J.C., Oudkerk, M., Witteman, J.C.M., Hofman, A., Van Gijn, J., Breteler, M.M.B., 2002. Hypertension and cerebral white matter lesions in a prospective cohort study. *Brain* 125, 765–772.
- Debette, S., Markus, H.S., 2010. The clinical importance of white matter hyperintensities on brain magnetic resonance imaging: systematic review and meta-analysis. *BMJ* 341, c3666.
- DeCarli, C., Fletcher, E., Ramey, V., Harvey, D., Jagust, W.J., 2005. Anatomical mapping of white matter hyperintensities (WMH): exploring the relationships between periventricular WMH, deep WMH, and total WMH burden. *Stroke* 36, 50–55.
- DeCarli, C., Miller, B.L., Swan, G.E., Reed, T., Wolf, P.A., Carmelli, D., 2001. Cerebrovascular and brain morphologic correlates of mild cognitive impairment in the national heart, lung, and blood institute twin study. *Arch. Neurol.* 58, 643–647.
- Dubois, B., Feldman, H.H., Jacova, C., Hampel, H., Molinuevo, J.L., Blennow, K., DeKosky, S.T., Gauthier, S., Selkoe, D., Bateman, R., 2014. Advancing research diagnostic criteria for Alzheimer's disease: the IWG-2 criteria. *Lancet Neurol.* 13, 614–629.
- Dufouil, C., de Kersaint-Gilly, A., Besançon, V., Levy, C., Auffray, E., Brunner, L., Alperovitch, A., Tzourio, C., 2001. Longitudinal study of blood pressure and white matter hyperintensities the EVA MRI cohort. *Neurology* 56, 921–926.
- Dufouil, C., Chalmers, J., Coskun, O., Besançon, V., Bousser, M.-G., Guillon, P., MacMahon, S., Mazoyer, B., Neal, B., Woodward, M., Tzourio-Mazoyer, N., Tzourio, C., 2005. Effects of blood pressure lowering on cerebral white matter hyperintensities in patients with stroke. *Circulation* 112, 1644–1650.
- Edwards, J.D., Ramirez, J., Callahan, B.L., Tobe, S.W., Oh, P., Berezuk, C., Lanctôt, K., Swardfager, W., Nestor, S., Kiss, A., Strother, S., Black, S.E., Alzheimer's Disease Neuroimaging Initiative, 2017. Antihypertensive treatment is associated with MRI-derived markers of neurodegeneration and impaired cognition: a propensity-weighted cohort study. *J. Alzheimers Dis.* 59, 1113–1122.
- Fazekas, F., Klei, R., Offenbacher, H., Schmidt, R., Kleinert, G., Payer, F., Radner, H., Lechner, H., 1993. Pathologic correlates of incidental MRI white matter signal hyperintensities. *Neurology* 43, 1683–1689.
- Fonov, V., Coupé, P., Eskildsen, S.F., Collins, L.D., 2011. Atrophy specific MRI brain template for Alzheimer's disease and mild cognitive impairment. *Alzheimers Dement* 7, S58.
- Fornari, E., Maeder, P., Meuli, R., Ghika, J., Knyazeva, M.G., 2012. Demyelination of superficial white matter in early Alzheimer's disease: a magnetization transfer imaging study. *Neurobiol. Aging* 33, 428.e7–428.e19.
- Gao, J., Cheung, R.T., Chan, Y.-S., Chu, L.-W., Mak, H.K., Lee, T.M., 2014. The relevance of short-range fibers to cognitive efficiency and brain activation in aging and dementia. *PLoS One* 9, e90307.
- Gouw, A.A., Seewann, A., Van Der Flier, W.M., Barkhof, F., Rozemuller, A.M., Scheltens, P., Geurts, J.J., 2010. Heterogeneity of small vessel disease: a systematic review of MRI and histopathology correlations. *J. Neurol. Neurosurg. Psychiatry* 82, 126–135.
- Griffanti, L., Jenkinson, M., Suri, S., Zsoldos, E., Mahmood, A., Filippini, N., Sexton, C.E., Topiwala, A., Allan, C., Kivimäki, M., 2017. Classification and characterization of periventricular and deep white matter hyperintensities on MRI: a study in older adults. *Neuroimage* 170, 174–181.
- Huang, C.-C., Yang, A.C., Chou, K.-H., Liu, M.-E., Fang, S.-C., Chen, C.-C., Tsai, S.-J., Lin, C.-P., 2018. Nonlinear pattern of the emergence of white matter hyperintensity in healthy Han Chinese: an adult lifespan study. *Neurobiol. Aging* 67, 99–107.
- Jellinger, K.A., Schmidt, R., Windisch, M. (Eds.), 2013. *Advances in Dementia Research*, Vol. 59. Springer Science & Business Media.
- Kandiah, N., Zainal, N.H., Narasimhalu, K., Chander, R.J., Ng, A., Mak, E., Au, W.L., Sitoh, Y.Y., Nadkarni, N., Tan, L.C., 2014. Hippocampal volume and white matter disease in the prediction of dementia in Parkinson's disease. *Parkinsonism Relat. Disord.* 20, 1203–1208.
- Kertesz, A., Black, S.E., Tokar, G., Benke, T., Carr, T., Nicholson, L., 1988. Periventricular and subcortical hyperintensities on magnetic resonance imaging: 'rims, caps, and unidentified bright objects'. *Arch. Neurol.* 45, 404–408.
- Kim, S., Choi, S.H., Lee, Y.M., Kim, M.J., Kim, Y.D., Kim, J.Y., Park, J.H., Myung, W., Na, H.R., Han, H.J., Shim, Y.S., Kim, J.H., Yoon, S.J., Kim, S.Y., Kim, D.K., 2015. Periventricular white matter hyperintensities and the risk of dementia: a CREDOS study. *Int. Psychogeriatr.* 27, 2069–2077.
- Kloppenburg, R.P., Nederkoorn, P.J., Geerlings, M.I., van den Berg, E., 2014. Presence and progression of white matter hyperintensities and cognition: a meta-analysis. *Neurology* 82, 2127–2138.
- Krishnan, M.S., O'Brien, J.T., Firbank, M.J., Pantoni, L., Carlucci, G., Erkinjuntti, T., Wallin, A., Wahlund, L.-O., Scheltens, P., van Straaten, E.C., 2006. Relationship between periventricular and deep white matter lesions and depressive symptoms in older people. The LADIS study. *Int. J. Geriatr. Psychiatry* 21, 983–989.
- Lee, H.K., Lee, Y.M., Park, J.M., Lee, B.D., Moon, E.S., Chung, Y.I., 2014. Amnesic multiple cognitive domains impairment and periventricular white matter hyperintensities are independently predictive factors progression to dementia in mild cognitive impairment. *Int. J. Geriatr. Psychiatry* 29, 526–532.
- National Academies of Sciences, Engineering, and Medicine, 2017. *Preventing Cognitive Decline and Dementia: A Way Forward*. National Academies Press.
- Li, J.-Q., Tan, L., Wang, H.-F., Tan, M.-S., Tan, L., Xu, W., Zhao, Q.-F., Wang, J., Jiang, T., Yu, J.-T., 2016. Risk factors for predicting progression from mild cognitive impairment to Alzheimer's disease: a systematic review and meta-analysis of cohort studies. *J. Neurol. Neurosurg. Psychiatry* 87, 476–484.
- Lindemer, E.R., Salat, D.H., Smith, E.E., Nguyen, K., Fischl, B., Greve, D.N., Alzheimer's Disease Neuroimaging Initiative, 2015. White matter signal abnormality quality differentiates mild cognitive impairment that converts to Alzheimer's disease from nonconverters. *Neurobiol. Aging* 36, 2447–2457.
- Lopez, O.L., Jagust, W.J., DeKosky, S.T., Becker, J.T., Fitzpatrick, A., Dulberg, C., Breitner, J., Lyketsos, C., Jones, B., Kawas, C., Carlson, M., Kuller, L.H., 2003. Prevalence and classification of mild cognitive impairment in the cardiovascular health study cognition study: part 1. *Arch. Neurol.* 60, 1385–1389.
- Manjón, J.V., Coupé, P., Martí-Bonmati, L., Collins, D.L., Robles, M., 2010. Adaptive non-local means denoising of MR images with spatially varying noise levels. *J. Magn. Reson. Imaging* 31, 192–203.
- Matsushita, K., Kuriyama, Y., Nagatsuka, K., Nakamura, M., Sawada, T., Omae, T., 1994. Periventricular white matter lucency and cerebral blood flow autoradiography in hypertensive patients. *Hypertension* 23, 565–568.
- Matsusue, E., Sugihara, S., Fujii, S., Ohama, E., Kinoshita, T., Ogawa, T., 2006. White matter changes in elderly people: MR-pathologic correlations. *Magn. Reson. Med. Sci.* 5, 99–104.
- McAleese, K.E., Alafuzoff, I., Charidimou, A., De Reuck, J., Grinberg, L.T., Hainsworth, A.H., Hortobagyi, T., Ince, P., Jellinger, K., Gao, J., 2016. Post-mortem assessment in vascular dementia: advances and aspirations. *BMC Med.* 14, 129.
- Moody, D.M., Bell, M.A., Challa, V.R., 1990. Features of the cerebral vascular pattern that predict vulnerability to perfusion or oxygenation deficiency: an anatomic study. *Am. J. Neuroradiol.* 11, 431–439.
- Nazeri, A., Chakravarty, M.M., Rajji, T.K., Felsky, D., Rotenberg, D.J., Mason, M., Xu, L.N., Lobaugh, N.J., Mulsant, B.H., Voineskos, A.N., 2015. Superficial white matter as a novel substrate of age-related cognitive decline. *Neurobiol. Aging* 36, 2094–2106.
- Petersen, R.C., Aisen, P.S., Beckett, L.A., Donohue, M.C., Gamst, A.C., Harvey, D.J., Jack, C.R., Jagust, W.J., Shaw, L.M., Toga, A.W., Trojanowski, J.Q., Weiner, M.W., 2010. Alzheimer's disease neuroimaging initiative (ADNI) clinical characterization. *Neurology* 74, 201–209.
- Prins, N.D., Scheltens, P., 2015. White matter hyperintensities, cognitive impairment and dementia: an update. *Nat. Rev. Neurol.* 11, 157–165.
- Shim, Y.S., Yang, D.-W., Roe, C.M., Coats, M.A., Benzinger, T.L., Xiong, C., Galvin, J.E., Cairns, N.J., Morris, J.C., 2015. Pathological correlates of white matter hyperintensities on magnetic resonance imaging. *Dement. Geriatr. Cogn. Disord.* 39, 92–104.
- Sled, J.G., Zijdenbos, A.P., Evans, A.C., 1998. A nonparametric method for automatic correction of intensity nonuniformity in MRI data. *Med. Imaging IEEE Trans.* 17, 87–97.
- Tosto, G., Zimmerman, M.E., Carmichael, O.T., Brickman, A.M., 2014. Predicting aggressive decline in mild cognitive impairment: the importance of white matter hyperintensities. *JAMA Neurol.* 71, 872–877.
- van den Berg, E., Geerlings, M.I., Biessels, G.J., Nederkoorn, P.J., Kloppenburg, R.P., 2018. White matter hyperintensities and cognition in mild cognitive impairment and Alzheimer's disease: a domain-specific meta-analysis. *J. Alzheimers Dis.* 63, 515–527.
- van Straaten, E.C., Harvey, D., Scheltens, P., Barkhof, F., Petersen, R.C., Thal, L.J., Jack, C.R., DeCarli, C., others, 2008. Periventricular white matter hyperintensities increase the likelihood of progression from amnesic mild cognitive impairment to dementia. *J. Neurol.* 255, 1302.
- Yoshita, M., Fletcher, E., DeCarli, C., 2005. Current concepts of analysis of cerebral white matter hyperintensities on magnetic resonance imaging. *Top. Magn. Reson. Imaging* 16, 399–407.